OAK RIDGE NATIONAL LABORATORY
operated by
UNION CARBIDE CORPORATION
for the
U. S. ATOMIC ENERGY COMMISSION

UNION CARBIDE

ORNL - TM - 2233

COPY NO. -

DATE - May 17, 1968

MAGNETIC FLUX FLOW AND SUPERCONDUCTOR STABILIZATION

W. F. Gauster, K. R. Efferson, J. B. Hendricks, D. M. Kroeger
M. S. Lubell, and J. E. Simpkins

Abstract

Our previously reported work has been continued during this fourth report period. The observations on the flux flow and stability performance of bare NbTi strips have been extended to include two additional compositions, viz Nb-5% Ti and Nb-10% Ti, which have similar critical temperatures but widely different upper critical fields and normal state resistivities. The results obtained with these samples confirm our previous conclusion that heat transfer phenomena rather than electrical effects (or a fortuitous interaction between electrical and heat transfer) were of primary importance in understanding premature take-offs. These results agree well with the observation on temperature fluctuations as described below. It has also been shown that the analysis of the field dependent recovery power can yield the heat flux as a function of temperature for the film boiling regime.

To improve the analysis on compound conductors, it is necessary to make direct measurements of the magnetoresistance of the stabilizer and of the critical temperature of the superconductor. A new environmental test cell constructed for this purpose is described.

Additional heat transfer measurements have been performed and reproducible fluctuations in the temperature of the heated sample in nucleate boiling have been observed. They increase in magnitude with the power dissipation and with the height of the liquid helium column above the sample. In the helium bath itself (without operating probes) temperature fluctuations are likewise observed. They are at least two orders of magnitude smaller and they also increase in magnitude with the height of the helium column. Finally, as anticipated, the thin film work has proved to be a useful tool for the manufacturing of new heat transfer probes.

MAGNETIC FLUX FLOW

AND SUPERCONDUCTOR STABILIZATION

Quarterly Report Covering the Period From

January 1, 1968 to March 31, 1968

Prepared for

George C. Marshall Space Flight Center

National Aeronautics and Space Administration

(Government Order No. H-29278A)

MAY 1968

By

Thermonuclear Division

Oak Ridge National Laboratory

Oak Ridge, Tennessee

(Operated by Union Carbide Corporation, Nuclear Division)

TABLE OF CONTENTS

MAGNETIC FLUX FLOW AND SUPERCONDUCTOR STABILIZATION

I. INTRODUCTION

This fourth quarterly report deals with investigations on the flux flow and stability performance of NbTi strips with 5, 10, and 25 atomic percent titanium. The data were analyzed to determine if the premature take-off was caused principally by electrical or heat transfer phenomena. Since these samples have very different electrical properties (upper critical field, flux flow and normal state resistances) and somewhat different dimensions, the probability for an accidental correlation between thermal and electrical effects was significantly reduced. Analysis of the recovery data yielded similar heat transfer characteristics in the film boiling regime for all three samples.

To continue our work on the analysis of the current-voltage characteristics of compound conductors in the current sharing state, it seemed to be desirable to make direct measurements of the magnetoresistance of the stabilizer and critical temperature measurements of the superconductor. Therefore, a new environmental test cell has been constructed.

In connection with our studies on bare NbTi ribbons it became interesting to investigate carefully temperature fluctuations in liquid helium. These investigations are described in the section on heat transfer measurements. A very useful tool for these measurements is a glass probe with a thin film metal resistance layer which contains a carbon resistor for the temperature measurements. Our newly developed thin film techniques proved to be very useful for manufacturing similar probes. The probe construction is described in detail.

II. FLUX FLOW AND STABILITY PERFORMANCE OF BARE NbTi STRIPS

M. S. Lubell and D. M. Kroeger

A. Introduction.

Flux flow studies similar to those performed on a Nb-25% Ti strip have been made on specimens rolled from ingots with the nominal compositions, Nb-5% Ti and Nb-10% Ti. This has enabled us to obtain relevant data on materials with similar critical temperatures (and only slightly different from that of Nb-25% Ti) but with significantly varying critical fields, normal state resistivities and critical current densities. While some differences in detail exist, the overall results on the 5 and 10% Ti alloys confirm the previously proposed ideas and explanations for the anomalous dependence of power dissipation at take-off on field. It will also be shown that analysis of the field dependent recovery power can give the heat flux as a function of temperature for the film boiling regime.

B. Flux Flow Data.

Figures 1 and 2 show typical flux-flow characteristics for the 5% Ti and 10% Ti samples. The field was perpendicular to both the current and the sample face and the voltage drop along a 1 cm segment was measured.

In both samples the V - I characteristics exhibited a linear region for most field values. The slope dV/dI in this linear region is what is known as the flux-flow resistance R_f. Figures 3 and 4 show a plot of ρ_f/ρ_n vs $H/H_{c2}(0)$, where ρ_f is the flux-flow resistivity determined from R_f, ρ_n is the normal state resistivity measured at 4.2 K in a field greater than H_{c2}, and $H_{c2}(0)$ is the upper critical field at T = 0. According to ideas developed by Kim et al.[1] an extrapolation of the linear part of a plot of ρ_f/ρ_n vs H reaches $\rho_f/\rho_n = 1$ at $H = H_{c2}(0)$. It was in this fashion

that $H_{c2}(0)$ was determined. As was remarked in a previous report[2] in connection with a plot of ρ_f/ρ_n vs $H/H_{c2}(0)$ for the 25% Ti sample, values of $\rho_f/\rho_n > 1$ are not inconsistent with the requirement that $(V/I)_{ff} < R_n$ for all fields up to H_{c2}, since ρ_f is a differential resistivity.

In Table I are given measured parameters and pertinent information for all three samples, along with calculated values of the Ginsburg-Landau parameter κ and γ, the electronic-specific heat coefficient. The cross sectional area is designated by A and the total surface area between voltage contacts by S. Both γ and κ were calculated from the GLAG theory in the dirty limit,[3] $\gamma = 3.2 \times 10^{-5} \left[H_{c2}(0)/\rho_n T_c\right]$ and $\kappa = 0.29 \left[H_{c2}(0)/\gamma^{\frac{1}{2}} T_c\right]$.

Figure 5 shows a comparison for the three compositions of critical current density versus reduced field H/H_{c2}. Note that all three have a peak in critical current density, although its position and size vary considerably with composition, as does the general magnitude of J_c. However, a discussion of these points has not been the object of this study. The two additional compositions with widely differing values for such electrical parameters as ρ_n, H_{c2}, and J_c were studied to avoid erroneous overemphasis on the role of heat transfer in the data of the 25% Ti sample. The results obtained with these samples confirm our previous conclusion that heat transfer phenomena rather than electrical effects were of primary importance in understanding premature take-offs.

C. Recovery Power.

In a previous quarterly progress report,[4] we discussed the fact that the recovery power data of the Nb-25% Ti sample at low fields could be analyzed to deduce the heat transfer characteristics in the film boiling region between a solid surface and liquid helium. This discussion can now

be continued and the data necessary for the analysis and resulting heat transfer diagrams for all three compositions will be shown.

After a take-off (or an abrupt transition to the normal state) has been reached, the heat transfer characteristics which apply are those of film boiling. On reducing the power (by a decrease in current), the transition back to the flux flow state can be determined either by reaching the power associated with the minimum heat flux in film boiling, $\dot{q}_f$, with a corresponding $\Delta T = \tau_f$ or by passing through the field dependent critical temperature, $\tau_c(H) > \tau_f$ -- thus undergoing a normal-to-superconducting transition. The decrease in power associated with the transition to flux flow results in a return to nucleate boiling. These ideas will be made clearer by considering Fig. 6, along with the recovery point data. The return point data for the Nb-5% Ti and the Nb-10% Ti samples are shown in Fig. 7 and Fig. 8, respectively. The Nb-25% Ti data was shown in Ref. 4, p. 28.

At high fields ($> H/H_{c2} \simeq 0.5$ for the 5% and 10% samples and $> H/H_{c2} \simeq 0.6$ for the 25% sample), P_r was approximately constant. In this region, the transition out of the normal state was due to a film to nucleate boiling transition at $\dot{q}_f$ ($= 0.45 \pm 0.02$ W/cm^2) which reduced the sample temperature below the critical temperature for that field; hence, the sample returned to the flux flow state. In Fig. 6, an idealized heat transfer diagram, log $\dot{q}$ vs log τ, is shown. The above ideas are based on a film to nucleate boiling transition temperature, τ_f larger than $\tau_c(H_1)$ $\left[= T_c(H_1) - T_B\right]$, the normal to superconducting transition temperature associated with high fields. For simplicity, only one transition temperature is indicated. In fields below approximately $H_{c2}/2$ for the 5% and 10% samples and $3H_{c2}/5$ for the

25% specimen, the above condition is no longer valid but rather one can assume that the superconducting transition temperature $\tau_c(H_2)$ $\left[= T_c(H_2) - T_B\right]$ is above the film-to-nucleate boiling transition temperature, τ_f. In this case, when the sample was in the normal state in film boiling and the power to the sample was decreased (by decreasing the current), the sample temperature decreased in accordance with the $\dot{q}$ vs τ for the film boiling regime of the heat transfer characteristic. If the temperature of the sample should be reduced below its critical temperature, $\tau_c(H_2)$, before the minimum heat flux in film boiling, τ_f, is reached, then the normal-to-superconducting flux flow transition would occur first; and, as a consequence of the reduced heat production, the film-to-nucleate boiling transition would follow closely. For this hypothesis to be true, the power level at recovery would be larger at low fields where the transition temperature is also largest. This is true, as shown in Figs. 7 and 8 and Fig. 5, Ref. 4. Using the above ideas, the straight line through the data points at low fields was combined with the dependence of H_{c2} on T to yield an expression for $\dot{q} = f(\tau)$ for the film boiling region. Although we do not have a measurement of this region for our material and geometry, it is nevertheless encouraging that the derived film boiling curve lies between the data of Lyon[5] and Eastman and Datars.[8]

From the data in Figs. 7 and 8 and similarly for the 25% sample, the power dependence on field is obtained

$$\dot{q} = -mH_{c2}(T) + P_r(T_c) \quad , \tag{1}$$

where $P_r(T_c)$ is the power corresponding to the zero field transition temperature. A quadratic dependence of H_{c2} on T was found to best fit the available data for the Nb-5% Ti and the Nb-10% Ti samples and this is

shown in Figs. 9 and 10, respectively. A 3/2 power law was necessary for approximating the data of the Nb-25% Ti as shown in Fig. 11. For the 5 and 10% samples then,

$$H_{c2}(T) = H_{c2}(0)\left[1 - (T/T_c)^2\right] \quad . \tag{2}$$

Substituting the necessary parameters from Table I, $H_{c2}(0)$ and T_c and $T = \Delta T + T_B$ and combining Eqs. (1) and (2) enable one to calculate $\dot{q}$ as a function of ΔT. A plot of log $\dot{q}$ vs log ΔT with $T_b = 4.2$ K is shown in Fig. 12 for both the 5% and 10% samples. In Fig. 13, a similar graph is shown for the Nb-25% Ti strip derived in the same manner as the other compositions, except for the substitution of a 3/2 power for the square dependence in Eq. (2). For all three alloys, the temperature dependence of the heat transfer was linear and of the form

$$\dot{q} = 0.039\ \Delta T + \text{constant} \quad . \tag{3}$$

This linear temperature dependence for the film boiling regime agrees with Dory,[7] while Lyon[5] and Cummings and Smith[8] both give $\dot{q} \propto \Delta T^{0.92}$. The Breen and Westwater[9] correlation gives for tubes with surface areas comparable to our strips $\dot{q} = 0.09\ \Delta T$ + constant. Since our method of measurement was not sufficiently accurate to properly distinguish between these two values of the exponent, the question of whether our method agrees or disagrees with conventional heat transfer measurements remains open.

Owing to the fact that surface position relative to the bath is known to be important,[5] it was considered useful to compare the recovery data of a "sideways" position with the above data taken with the sample in a position having a "top" and "bottom" to determine the effect of geometry on film boiling. Accordingly, the Nb-10% Ti sample was rotated about its long

axis so that the field was parallel to the faces but still perpendicular to the current. The recovery power data for this geometry is shown in Fig. 14. Proceeding in a similar manner as discussed above, the power vs ΔT was calculated and is shown in Fig. 15 along with the perpendicular case for comparison. The heat transfer can be fit to a linear temperature dependence in this case also, but the slope is changed as well as the intercept. The form of the sideways case is

$$\dot{q} = 0.02\ \Delta T + \text{constant} \quad . \tag{4}$$

While this analysis and technique may not provide heat transfer data as accurate as the conventional heat transfer measurements where the temperature is measured directly, it nevertheless raises the interesting possibility of being a useful tool to investigate unusual or difficult geometries should the need arise.

Comparing the results of Lyon[5] with the above data on the minimum heat flux in film boiling leads to an interesting speculation. For the "sideways" geometry, Lyon found the maximum heat flux in nucleate boiling of 0.6 W/cm^2 which is the value of the minimum heat flux in film boiling for our Nb-10% Ti sample. For the "top" and "bottom" geometry, Lyon found for the mean value 0.5 W/cm^2, which is approximately 0.05 W/cm^2 larger than our $\dot{q}_f$ for all three samples. Our results then are consistent with Lyon's flat plate data under the condition that there is essentially no hysteresis between the nucleate and film boiling regimes. This conclusion of little hysteresis is further supported by recent measurements on stainless steel which also has poor thermal conductivity and low heat capacity.[4] (See also Sec. IV.)

D. V - I Anomaly.

Another interesting feature of these samples with small heat capacity was an anomalous V - I characteristic, which appeared just after the onset of flux flow at low power levels. A typical example of the anomaly which most often manifests itself by a "bump" in voltage is illustrated in Fig. 16. The power dissipation at the onset of the anomaly (2.2 A and 1 mV) was approximately 4.5 mW/cm^2. For other field values where this characteristic was observed, power dissipation was approximately of the same magnitude. Reeber[10] has shown that the change from convective cooling to nucleate boiling at a bath temperature of 4 K occurs over the range 1 to 10 mW/cm^2; Dory[7] gives the values between 1 to 5 mW/cm^2. Also, Reeber shows that there is a decided hysteresis in the superheat (increasing power has larger ΔT) for all bath temperatures in which the measurements were performed. We suggest that the voltage anomaly is a manifestation of the change from convective cooling to nucleate boiling -- thus emphasizing the importance of heat transfer even at very low power levels.

E. Take-Off Power.

Figures 7 and 8 show graphs of take-off power P_t and recovery power P_r versus applied field perpendicular to the sample surface for the 5% Ti and 10% Ti samples, respectively. Note that the take-off curves are quite different for the two compositions, and a comparison with P_t vs H for the 25% Ti material from a previous report[4] shows that the curve for this material is different from either of these. Graphs of P_t vs I_t for the 5% Ti and 10% Ti materials are shown in Figs. 17 and 18. A similar curve for the 25% Ti material was used in the previous report[11] to explain our ideas concerning the cause of take-off and the relationship between minimum

propagating current and take-off current. The P_t vs I_t curves for the three materials are not similar in detail, but the features of the curve for the 25% Ti sample which were important to our explanations are present also in the curves for the 5% Ti and 10% Ti samples. In particular, take-off does not occur for sample currents less than $\sim(\dot{q}_f s/R_n)^{\frac{1}{2}}$ where $\dot{q}_f$ is the minimum heat flux in film boiling determined from recovery data, and there is a significant change in character of the curves at I_t such that $I_t^2 R_n/S \sim 0.8$ W/cm^2. Measurements of the minimum propagating current I_p as a function of field for the 25% Ti sample were discussed in the last report. These measurements support the idea that the maximum value of $I_p(H)$ is such that $I_p^2 R_n/S = 0.8$ W/cm^2. Measurements of I_p for the other compositions have not yet been made, but the P_t vs I_t curves for these samples suggest that the same will be true for them.

As was reported previously for the 25% Ti sample, the transition from nucleate to film boiling for the 5% Ti and 10% Ti samples appears to occur at about 0.5 W/cm^2 instead of the 0.8 W/cm^2 which the P_t vs I_t curve might lead one to expect. We are thus led to speculate that the value of heat flux 0.8 W/cm^2 has a significance in relation to the heat transfer curve which is masked by the occurrence of the heat transfer fluctuations discussed in the previous report.

III. CURRENT-VOLTAGE CHARACTERISTICS OF COMPOUND CONDUCTORS

J. B. Hendricks

In the analysis of current-voltage characteristics of compound conductors in the current sharing state (flux flow state of the superconductor) the knowledge of the value of the stabilizer resistance, R, is necessary in order to separate the current into its superconductor and stabilizer components. In our previous work we have found R from the recovery points (observed in short sample experiments). In many cases, the results obtained in this way are only approximate. Therefore, we are building an apparatus to make a direct measurement of R as a function of temperature and external field.

The apparatus can also be used to find the critical temperature T_c vs magnetic field for wire samples. This parameter T_c is employed in our analysis of the current sharing state, and it would be desirable to know its exact value.

A part of the experimental apparatus is represented in Fig. 19. The piece shown is enclosed in a sealed can, which is immersed in liquid helium and evacuated by an oil diffusion pump to less than 1×10^{-6} mm Hg pressure. The only appreciable thermal contact between the copper parts and the liquid helium bath is through the two sample current leads. The sample potential leads, heater current leads, thermometer current and potential leads, and the stainless steel support tubes all have negligible heat leaks compared with sample current leads. Therefore, the temperature of the two copper heat sinks is set by the balance between heater input and heat leaking down the sample current leads. For #18 B&S copper leads $5\frac{1}{2}$" long, the heat leak is approximately 350 mW.

The two copper heat sinks, each of which is connected to one current lead, are insulated from the heater block with a 0.0005" thick mylar sheet. The mylar is covered with silicone vacuum grease to improve the heat contact. Two nylon screws hold the three copper pieces in tight contact.

The heater is wound of 12" of formvar coated #40 B&S NiCu wire with a room temperature resistance of 35Ω. After winding, the heater was coated with GE 6031 varnish to improve thermal contact.

The sample is bent into a circle 1.5" in diameter and soldered to the heat sinks. Potential leads are soldered to the sample and brought through the vacuum wall, the helium bath, to room temperature, and to the potentiometer terminals with no joints. Since the sample current is about 1 amp, and the sample resistance only 10μΩ, great care must be taken to minimize any thermal EMF's, such as would be present at joints.

Temperature is measured with a Texas Instruments, Inc. low temperature germanium thermometer. Its calibration accuracy from 4.2 K to 20 K is given as ±0.05% or ±0.1 K, whichever is greater. The thermometer resistance is measured with a standard four-terminal bridge.

The vacuum can, containing the experimental apparatus, fits inside a 2.1" bore, 8" long, 50 kG, 6th order corrected, stabilized NbTi superconducting magnet. The field homogeneity is calculated to be 0.01% over a 2" diameter sphere. The superconducting coil, with its small noise level, is required because of the very small EMF's being measured.

A preliminary model of the apparatus has been constructed and operated for a short time. Unfortunately, after a few cycles the feed-throughs in the vacuum can (kovar-glass seals) started leaking. These are now being replaced with epoxy seals, and the apparatus should be back in operation soon.

IV. MEASUREMENTS OF HEAT TRANSFER TO LIQUID HELIUM

K. R. Efferson and W. F. Gauster

In the previous report[11] it was mentioned that an experimental arrangement with a thin heat producing layer of low thermal conductivity (as in the case of a thin walled stainless steel tube which has been used for our experiments) tends to show thermal instabilities. Another experimental arrangement (using high thermal conducting material) is being prepared which is expected to dampen these thermal instabilities; thus, it would be possible to obtain smooth heat flux-temperature diagrams as needed for our flux flow investigations on commercially available compound conductors.

Our experiments with bare NbTi strips indicated the occurrence of thermal instabilities which influence the take-off currents of these samples. These observations show the importance of temperature instabilities in connection with these investigations. Therefore, we will discuss here certain details of the temperature instabilities observed during our heat transfer experiments with stainless steel tubes which have low thermal conductivity and heat capacity similar to bare NbTi strips.

Our recent experiments have been described in the preceding quarterly report,[11] page 11. A cylindrical sample in the form of a stainless steel tube of 2.5 mm outside diameter and 0.05 mm wall thickness has been used. A current I flowing through the tube produces heat which is dissipated to the surrounding liquid helium and the temperature of the inside surface of the tube is measured by means of a calibrated carbon resistor. The temperature at the outside tube surface can be calculated from the inside temperature and the sample current I. (See Ref. 4, page 15.)

Figure 20 shows the voltage drop V across the carbon resistor as ordinate and the sample current I as abscissa. The temperature T_i of the inside

surface of the tube is related to the voltage drop V across the carbon resistor. V and T_i scales are shown. The heat $\dot{q}$ dissipated per unit area is proportional to the square of I and a W/cm^2 scale is shown on top of Fig. 20. The liquid helium temperature was kept at 4.0 K by pumping. During the measurements, the liquid helium level (which was at the beginning of the experiment 30 cm above the sample) dropped by about 7 cm. Therefore, an average liquid helium column of 26.5 cm can be assumed.

This experiment was repeated with the same temperature of 4.0 K, however, with an average liquid helium column of only 4 cm (see Fig. 21). The temperature fluctuations are greatly reduced. This obvious influence of the height of the liquid helium column on the temperature fluctuation has been verified by repeated runs with different liquid helium columns.

Temperature fluctuations in pumped liquid helium (without a heated sample) have been observed.[12] We used carbon resistors arranged about 2.5 cm below the sample in order to monitor the temperature of the liquid helium. With zero sample power, fluctuations of the bath temperature were observed. The amplitude of these temperature fluctuations seemed to depend on the height of the liquid helium column in a similar manner as the sample temperature fluctuations (i.e., the amplitudes increased with the height, see Figs. 22a and 22b). It must be considered that the amplitudes of the bath temperature fluctuations are several orders of magnitude smaller than those of the sample.

Additional experiments will be made to investigate the performance with varying degrees of pumping and to find the influence of stirring the liquid helium bath.

V. THIN FILM DEVELOPMENTAL WORK

J. E. Simpkins

The vacuum deposition and the sputtering techniques which we are using for the production of thin films has been described in the previous reports, and several potential applications of these thin films for our research work in superconductivity have been mentioned. Recently, we employed the film technique for building a special probe for our heat transfer investigations (see Section IV).

The purpose of this probe is to generate electric power up to a few W/cm^2 at a cylindrical surface of about 3 mm diameter and about 10 cm length. A convenient resistance material seems to be a metal film about 1,000 Å thick. Our first attempt was to produce a copper film by vacuum deposition. This technique has the advantage that the copper film does not oxidize due to the moisture retained in the glass tubing since the glass surface is not heated during film deposition. Another advantage is that the deposition rate and film thickness may be controlled very closely.

The completed assembly of the probe is shown in Fig. 23. The 1/8" diameter pyrex tubing is sealed on one end. Thick copper contact areas are deposited on the glass tubing on both ends for soldering current and voltage leads. A copper "Housekeeper Seal" is attached to one end of the tubing, together with a copper plug and two copper tubes. One of these tubes, containing the lead wires, is sealed with epoxy, while the other is used to evacuate the pyrex tubing. After evacuation it is pinched off to form the final vacuum seal. The entire assembly is approximately 4" in length. Before the copper plug is soldered into position, a 1/10 watt 50 ohm carbon resistor, which is used to measure temperature on the inside

surface of the glass tubing, is placed inside the tube together with its current and voltage leads. Good thermal contact is made with GE 7031 insulating varnish. Pump-out holes are provided around the resistor to enable evacuation of the lower region of the tube.

As mentioned previously, this probe will be used for our heat transfer experiments. It might be of interest to operate this tube with other films. It should be possible to remove the copper film without damaging the probe and to vacuum deposit a copper film of different thickness or to apply a film of another material.

REFERENCES

1. Y. B. Kim, C. F. Hempstead, and A. R. Strnad, Phys. Rev. 139, A1163 (1965).
2. W. F. Gauster et al., ORNL-TM-1943, Aug. 9, 1967.
3. T. G. Berlincourt, Rev. Mod. Phys. 36, 19 (1964).
4. W. F. Gauster et al., ORNL-TM-2075, Dec. 1, 1967.
5. D. N. Lyon, Int. Adv. in Cryog. Eng. 10, 371 (1965).
6. P. C. Eastman and W. R. Datars, Cryogenics 3, 40 (1963).
7. A. P. Dory, Cryogenics 5, 146 (1965).
8. R. D. Cummings and J. L. Smith, Bull. Inst. Intern. Froid. Annexe 5, 85 (1966).
9. For Breen and Westwater and other correlations see E. G. Brentari and R. V. Smith, Adv. in Cryog. Eng. 10, 325 (1965).
10. M. D. Reeber, J. Appl. Phys. 34, 481 (1963).
11. W. F. Gauster et al., ORNL-TM-2162, March 1, 1968.
12. R. T. Swim, Adv. in Cryog. Eng. 5, 498 (1960).

TABLE CAPTION

Table I. Measured and Calculated Parameters for NbTi Alloys.

FIGURE CAPTIONS

Fig. 1 Flux flow voltage vs current at T_b = 4.2 K as a function of transverse field for a Nb-5% Ti strip.

Fig. 2 Flux flow voltage vs current at T_b = 4.2 K as a function of transverse field for a Nb-10% Ti strip.

Fig. 3 Normalized flux flow resistivity vs normalized transverse field at T_b = 4.2 K for a Nb-5% Ti strip.

Fig. 4 Normalized flux flow resistivity vs normalized transverse field at T_b = 4.2 K for a Nb-10% Ti strip.

Fig. 5 Comparison of the critical current density vs normalized transverse field at T_b = 4.2 K.

Fig. 6 An idealized heat transfer diagram log $\dot{q}$ vs log τ ($\tau = T - T_B$). The maximum nucleate boiling heat flux is $\dot{q}_n$ and $\dot{q}_f$ is the minimum heat flux in film boiling. $\tau_c(H_1) = T_c(H_1) - T_B$ is the transition temperature minus bath temperature associated with a high field while $\tau_c(H_2)$ is similarly associated with a low field.

Fig. 7 Take-off power, $P_t = V_t I_t$, and recovery power, $P_r = V_r I_r$, vs transverse field at T_b = 4.2 K for a Nb-5% Ti strip.

Fig. 8 Take-off power, $P_t = V_t I_t$, and recovery power, $P_r = V_r I_r$, vs transverse field at T_b = 4.2 K for a Nb-10% Ti strip.

Fig. 9 Upper critical field vs normalized temperature for Nb-5% Ti.

Fig. 10 Upper critical field vs normalized temperature for a Nb-10% Ti strip.

Fig. 11 Upper critical field vs normalized temperature for a Nb-25% Ti strip.

Fig. 12 Log of power vs log of temperature difference between surface and helium bath for the film boiling regime. Both curves are of the form $\dot{q} = 0.039\ \Delta T$ + constant.

Fig. 13 Log of power vs log of temperature difference between surface and helium bath for the film boiling regime. The curve is of the form $\dot{q} = 0.039\ \Delta T$ + constant.

Fig. 14 Recovery power, $P_r = V_r I_r$, vs parallel magnetic field. The field dependence of P_r is shown for $T_b = 4.2$ K.

Fig. 15 Log of power vs log of temperature difference between surface and helium bath for the film boiling regime at $T_b = 4.2$ K. The sample with field perpendicular has a "top" and "bottom" surface and with the field parallel it has two "sideways" surfaces.

Fig. 16 Voltage vs current at low power levels illustrating the anomaly and hysteresis at $T_b = 4.2$ K.

Fig. 17 Take-off power, $P_t = V_t I_t$, vs take-off current. Below $I_t = 4.4$ A and above $I_t = 5.85$ A dissipation in a normal zone was less than $\dot{q}_f$ and greater than $\dot{q}_n$, respectively.

Fig. 18 Take-off power, $P_t = V_t I_t$, vs take-off current. Below $I_t = 6.7$ A and above $I_t = 8.7$ A dissipation in a normal zone was less than $\dot{q}_f$ and greater than $\dot{q}_n$, respectively.

Fig. 19 Experimental apparatus for the measurement of resistance as a function of temperature.

Fig. 20 Heat flux-temperature diagram obtained with an average liquid helium column of 26.5 cm.

Fig. 21 Heat flux-temperature diagram obtained with an average liquid helium column of 4 cm.

Fig. 22 Temperature fluctuations in liquid helium pumped to 4.0 K.

(a) Average liquid helium column 29 cm;

(b) Average liquid helium column 6.5 cm.

Fig. 23 Thin film probe for heat transfer measurements.

TABLE I

Measured and Calculated Parameters for NbTi Alloys

	Nb-5% Ti	Nb-10% Ti	Nb-25% Ti
T_c [K]	9.2(a)	9.2(a)	10.5(b)
$H_{c2}(0)$ [kG]	19.5	38.5	100.0
ρ_n [$\mu\Omega$-cm]	8.4	13.5	31.2
H_{c2}(4.2K) [kG]	15.5	36.5	73.0
γ [k erg/cm^3-K^2]	8.0	10.0	10.0
κ	7.0	12.0	28.0
A [10^{-4} cm^2]	7.35	25.7	38.3
S [mm^2]	48.9	50.4	152.0

(a) W. A. Fietz and W. W. Webb, Phys. Rev. 161, 423 (1967).

(b) D. M. Kroeger, Ph.D. Thesis, Vanderbilt Univ., 1966 (unpublished).

(c) All other values were measured or calculated in the present work.

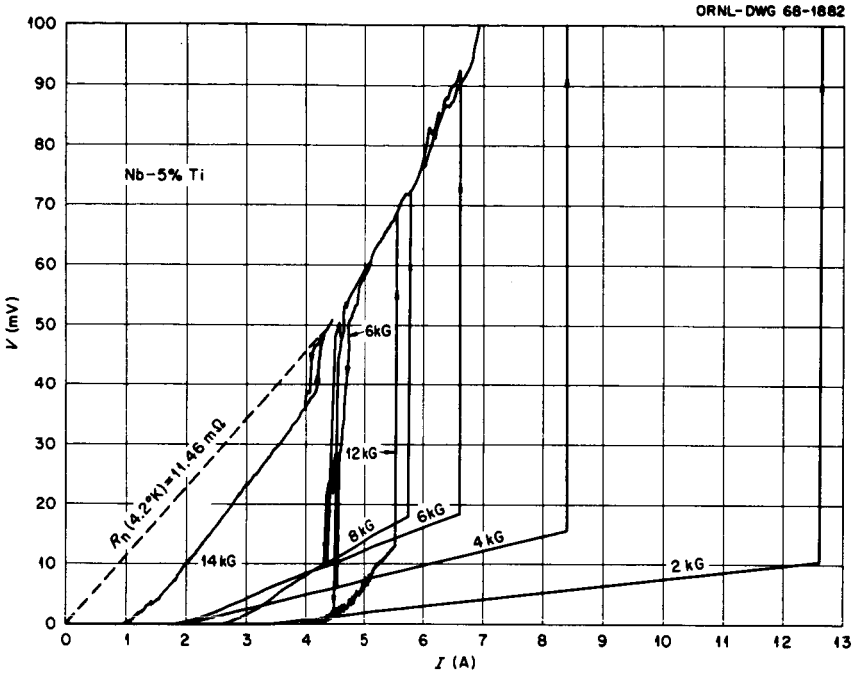

Fig. 1 Flux flow voltage vs current at T_b = 4.2 K as a function of transverse field for a Nb-5% Ti strip.

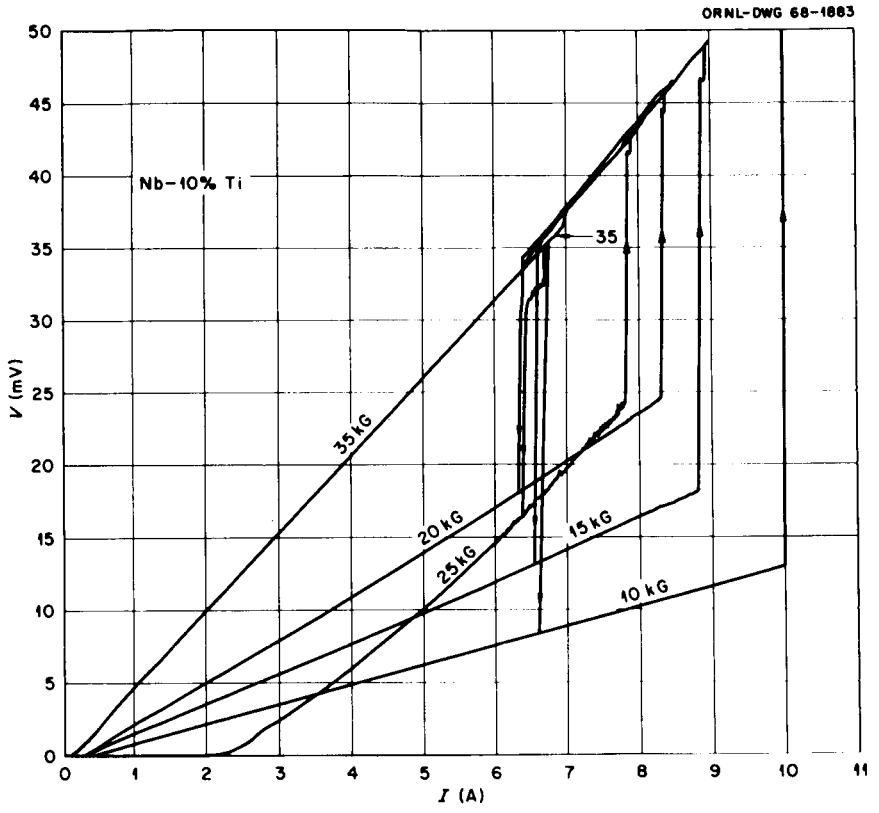

Fig. 2 Flux flow voltage vs current at T_b = 4.2 K as a function of transverse field for a Nb-10% Ti strip.

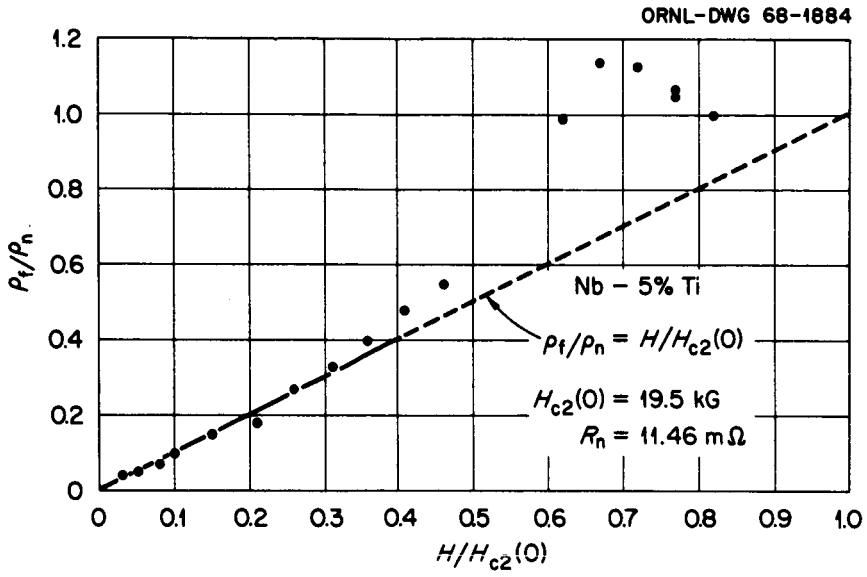

Fig. 3 Normalized flux flow resistivity vs normalized transverse field at T_b = 4.2 K for a Nb-5% Ti strip.

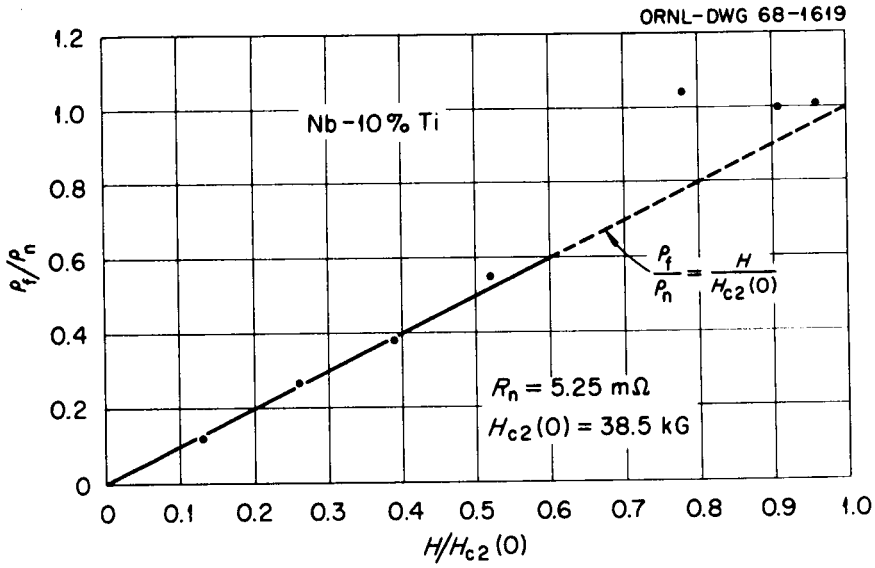

Fig. 4 Normalized flux flow resistivity vs normalized transverse field at T_b = 4.2 K for a Nb-10% Ti strip.

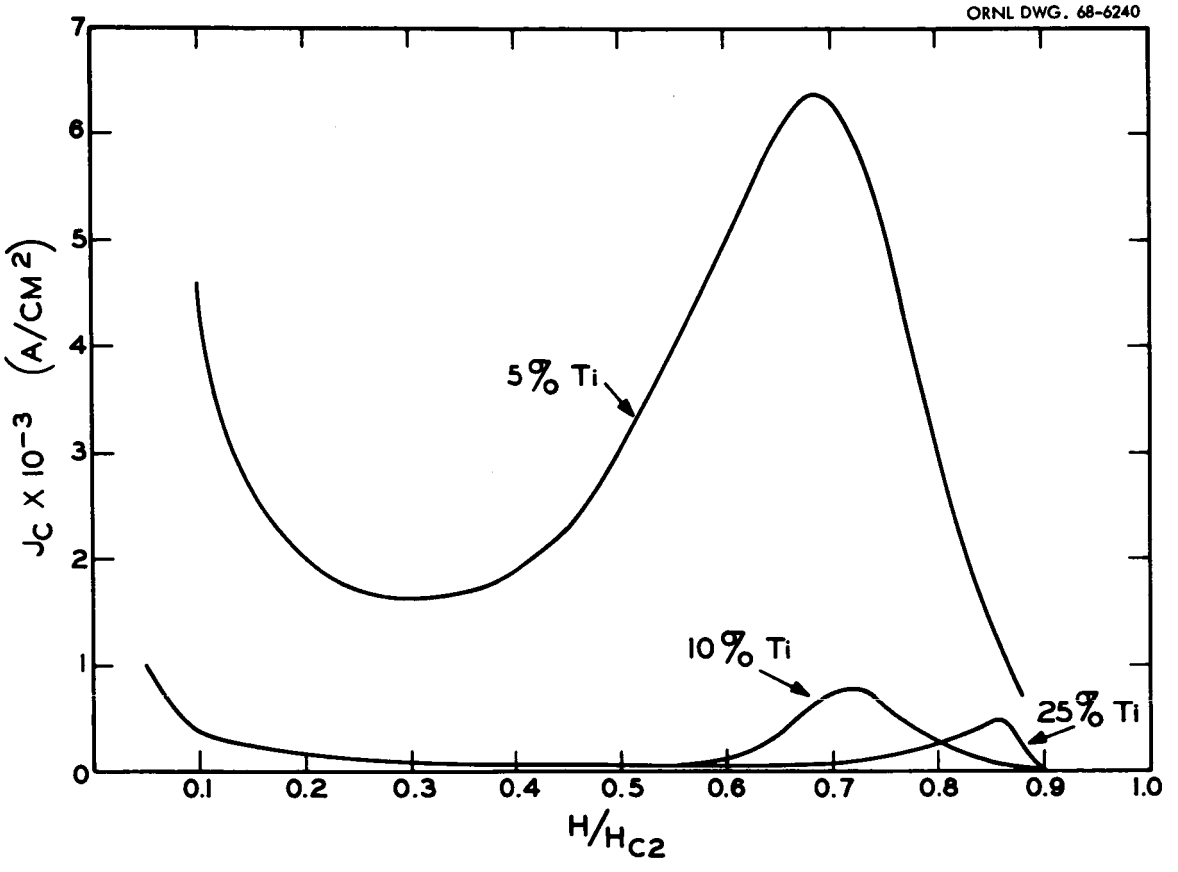

Fig. 5 Comparison of the critical current density vs normalized transverse field at T_b = 4.2 K.

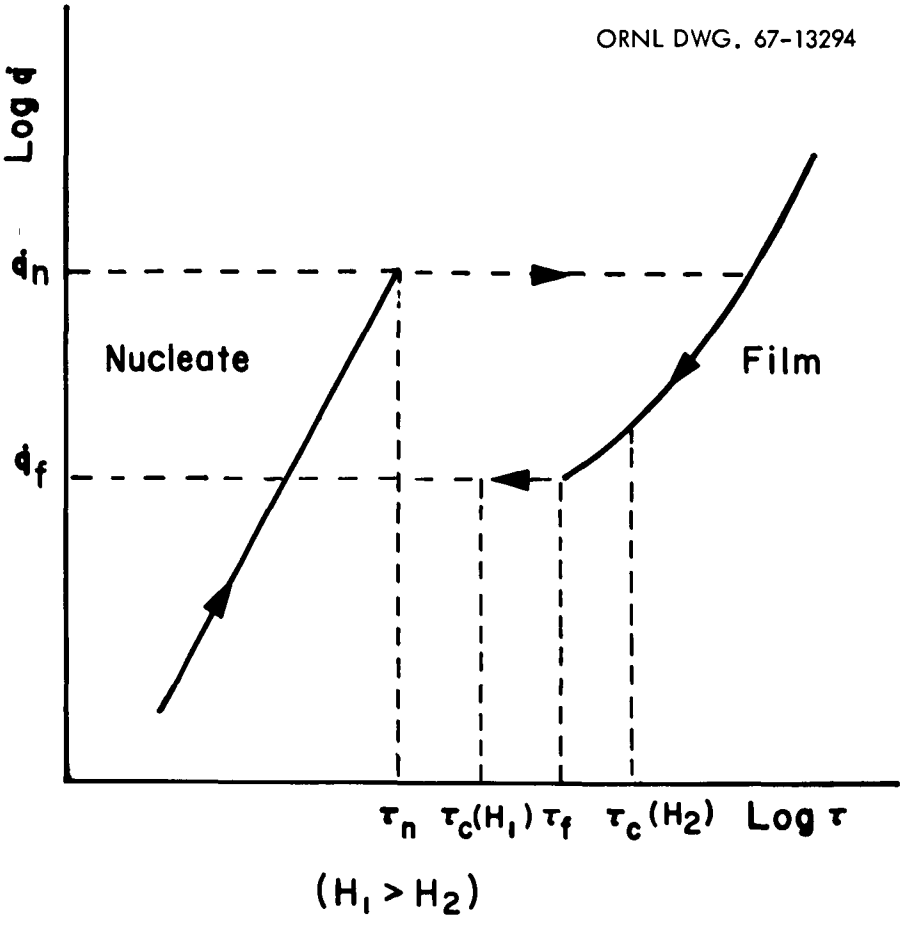

Fig. 6 An idealized heat transfer diagram log $\dot{q}$ vs log τ ($\tau = T - T_B$). The maximum nucleate boiling heat flux is $\dot{q}_n$ and $\dot{q}_f$ is the minimum heat flux in film boiling. $\tau_c(H_1) = T_c(H_1) - T_B$ is the transition temperature minus bath temperature associated with a high field while $\tau_c(H_2)$ is similarly associated with a low field.

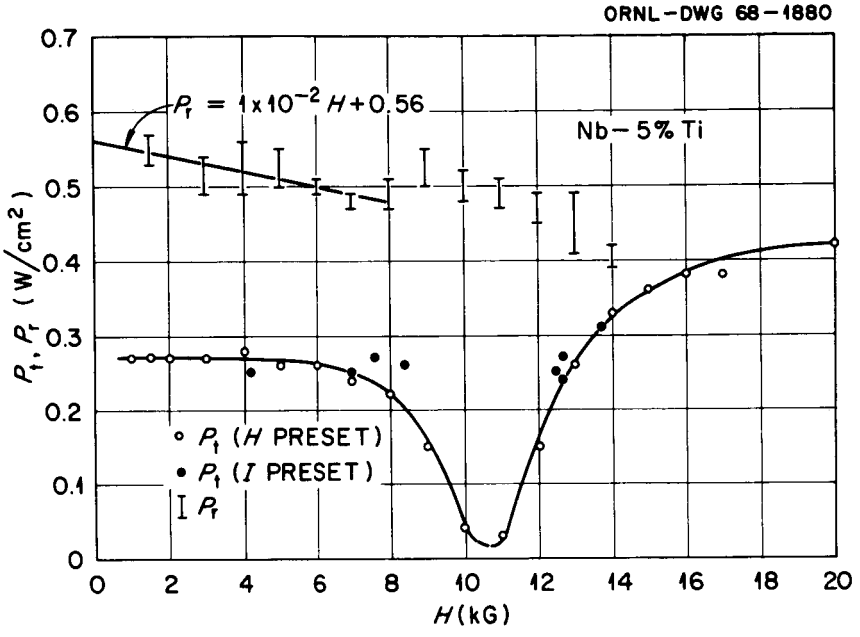

Fig. 7 Take-off power, $P_t = V_t I_t$, and recovery power, $P_r = V_r I_r$, vs transverse field at $T_b = 4.2$ K for a Nb-5% Ti strip.

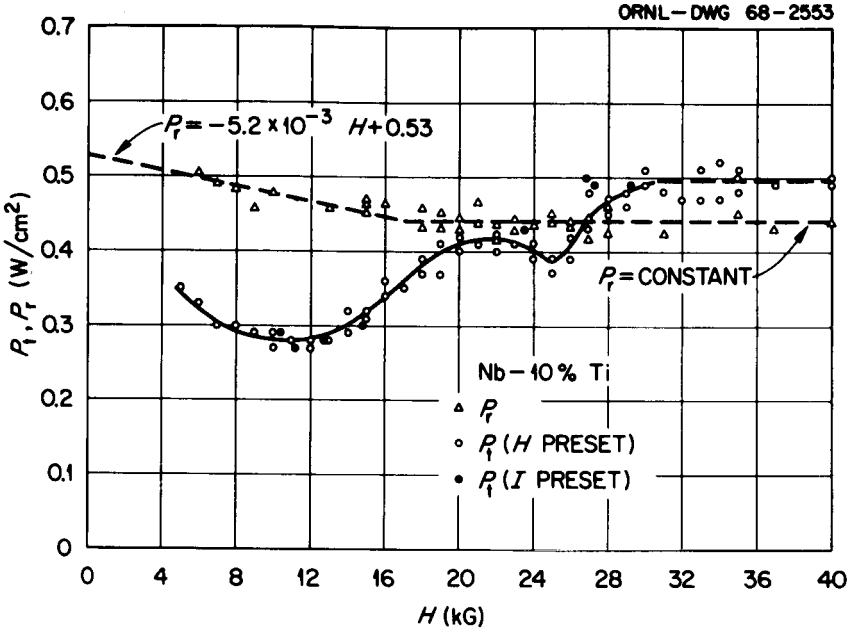

Fig. 8 Take-off power, $P_t = V_t I_t$, and recovery power, $P_r = V_r I_r$, vs transverse field at $T_b = 4.2$ K for a Nb-10% Ti strip.

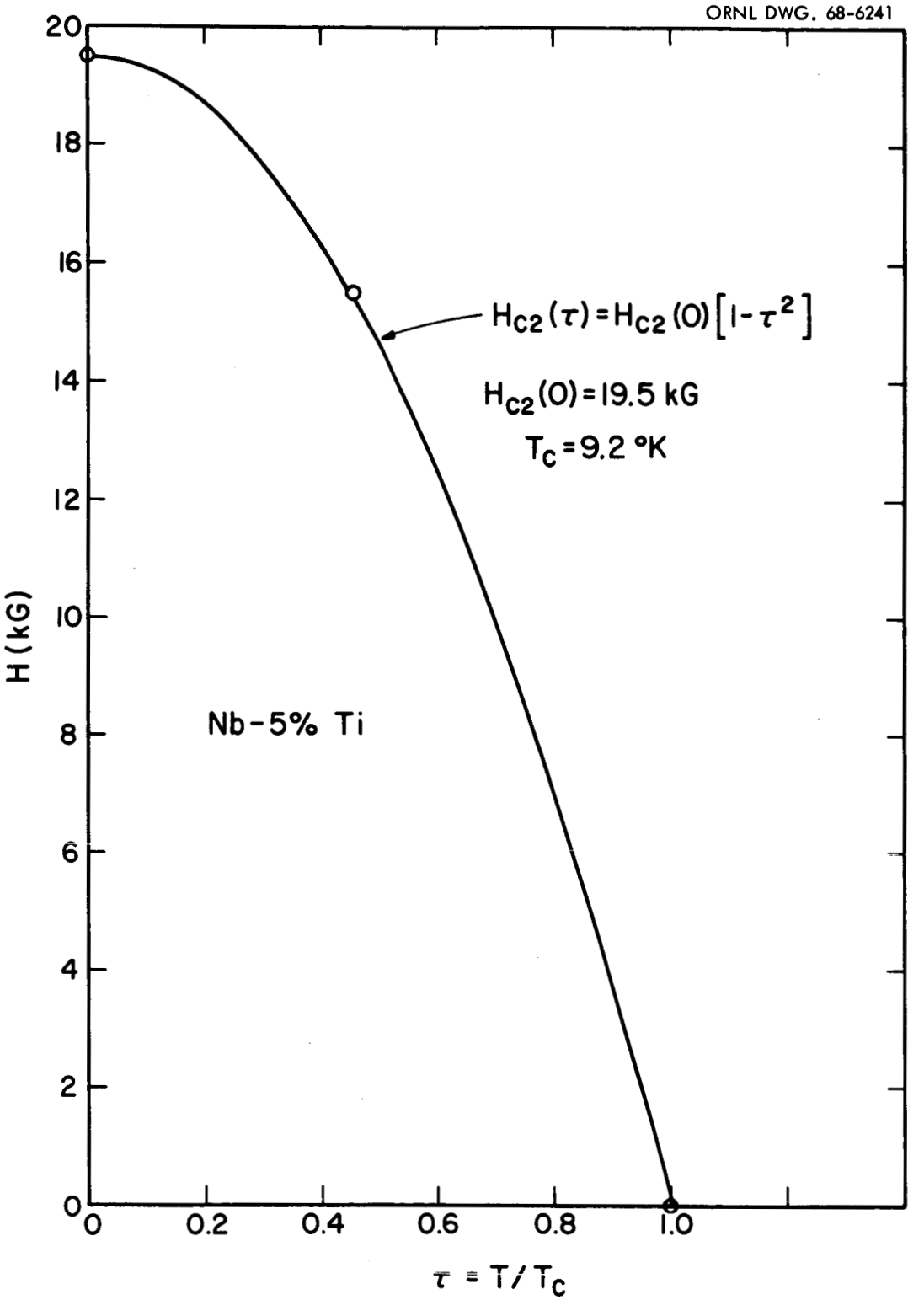

Fig. 9 Upper critical field vs normalized temperature for Nb-5% Ti.

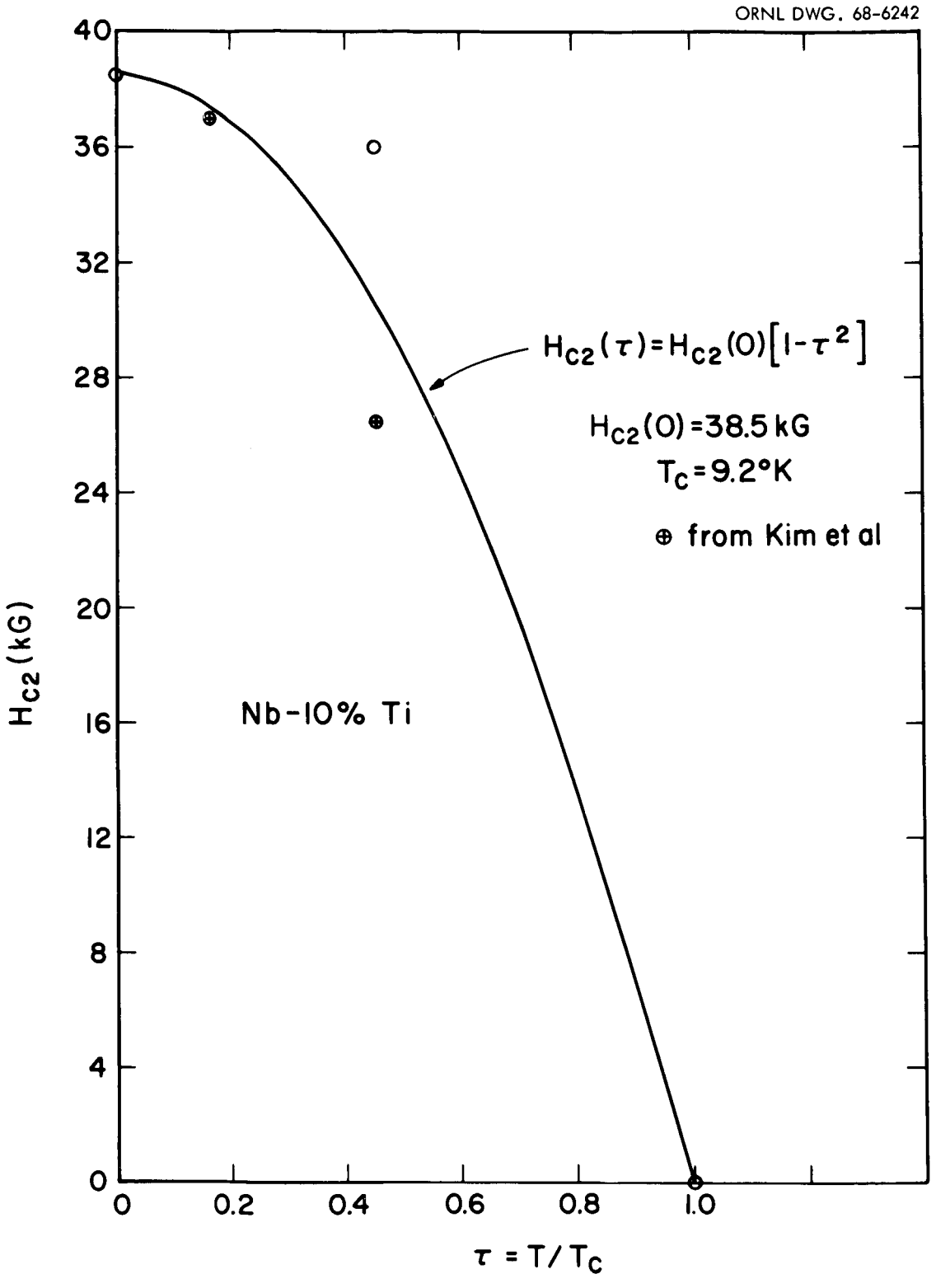

Fig. 10 Upper critical field vs normalized temperature for a Nb-10% Ti strip.

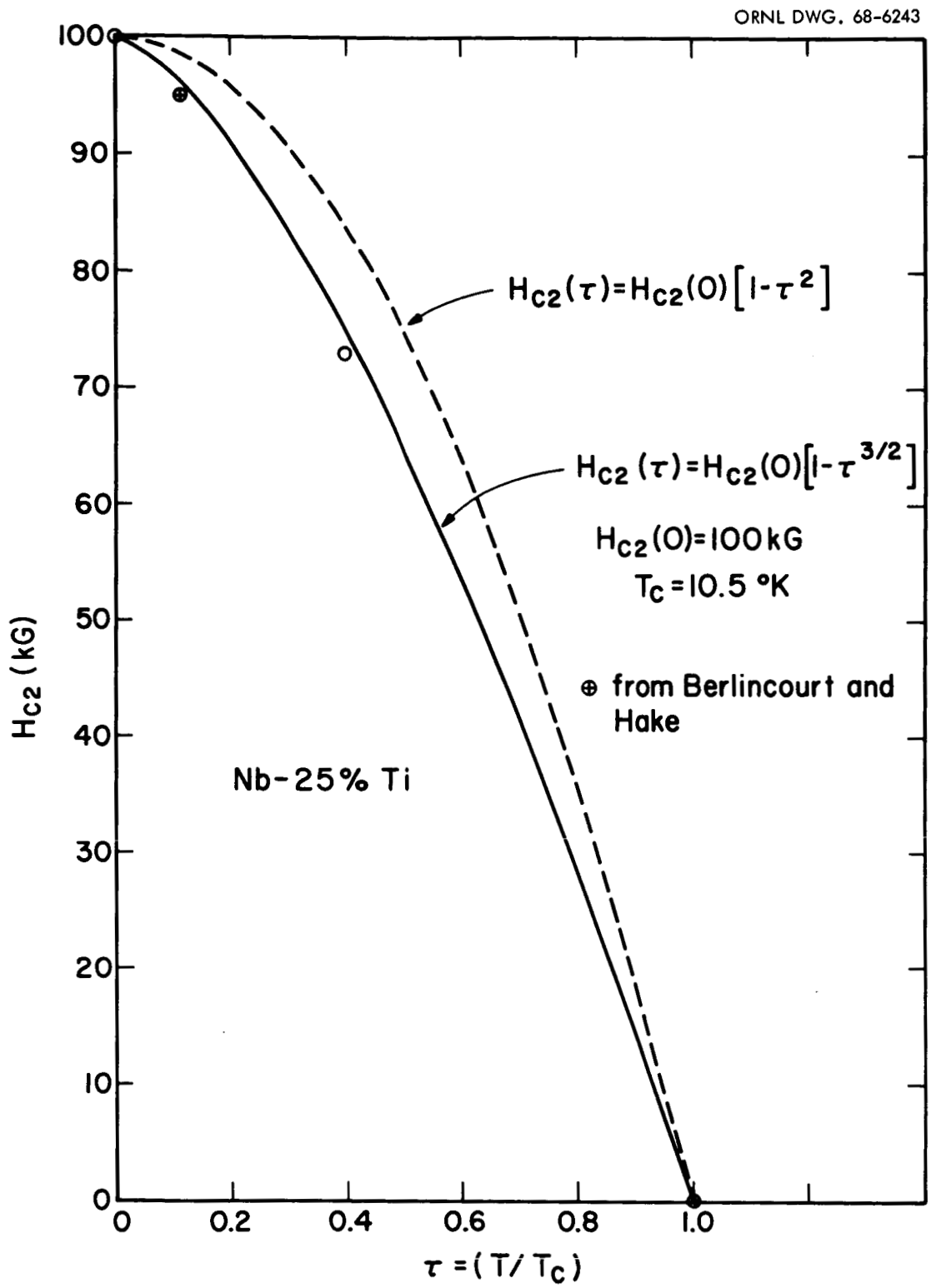

Fig. 11 Upper critical field vs normalized temperature for a Nb-25% Ti strip.

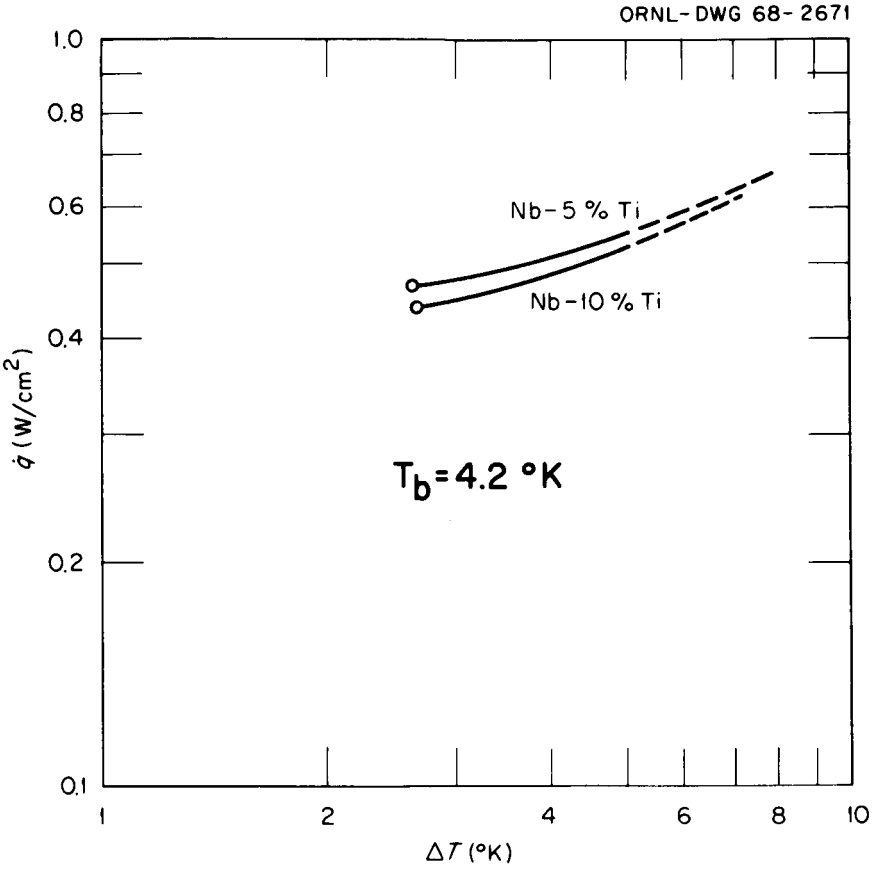

Fig. 12 Log of power vs log of temperature difference between surface and helium bath for the film boiling regime. Both curves are of the form $\dot{q} = 0.039\ \Delta T$ + constant.

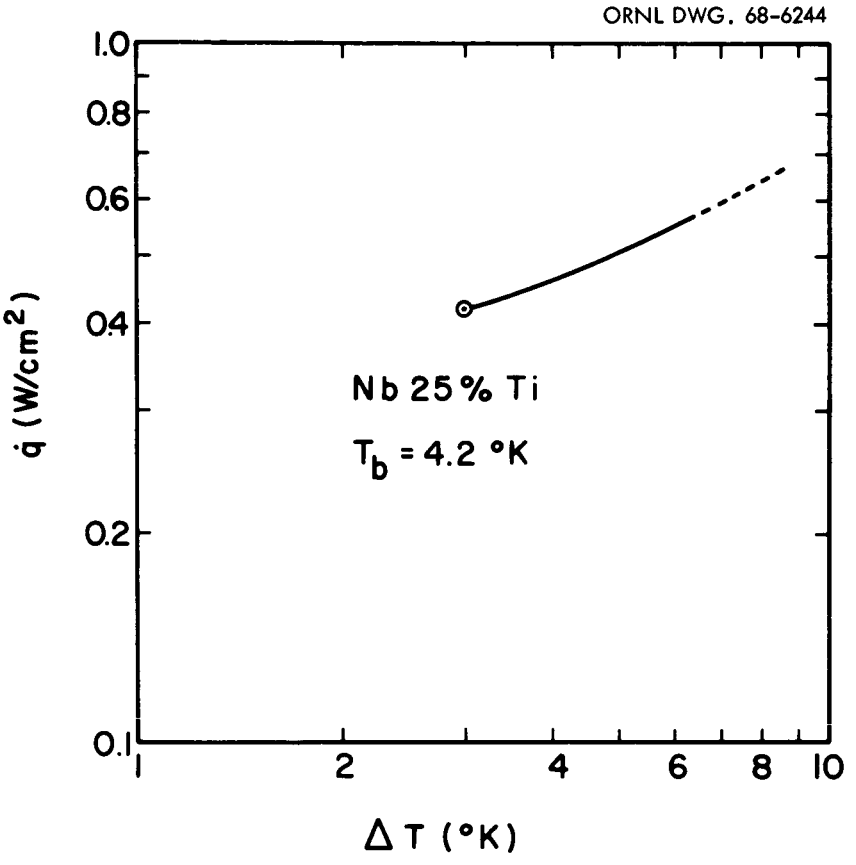

Fig. 13 Log of power vs log of temperature difference between surface and helium bath for the film boiling regime. The curve is of the form $\dot{q} = 0.039\ \Delta T + \text{constant}$.

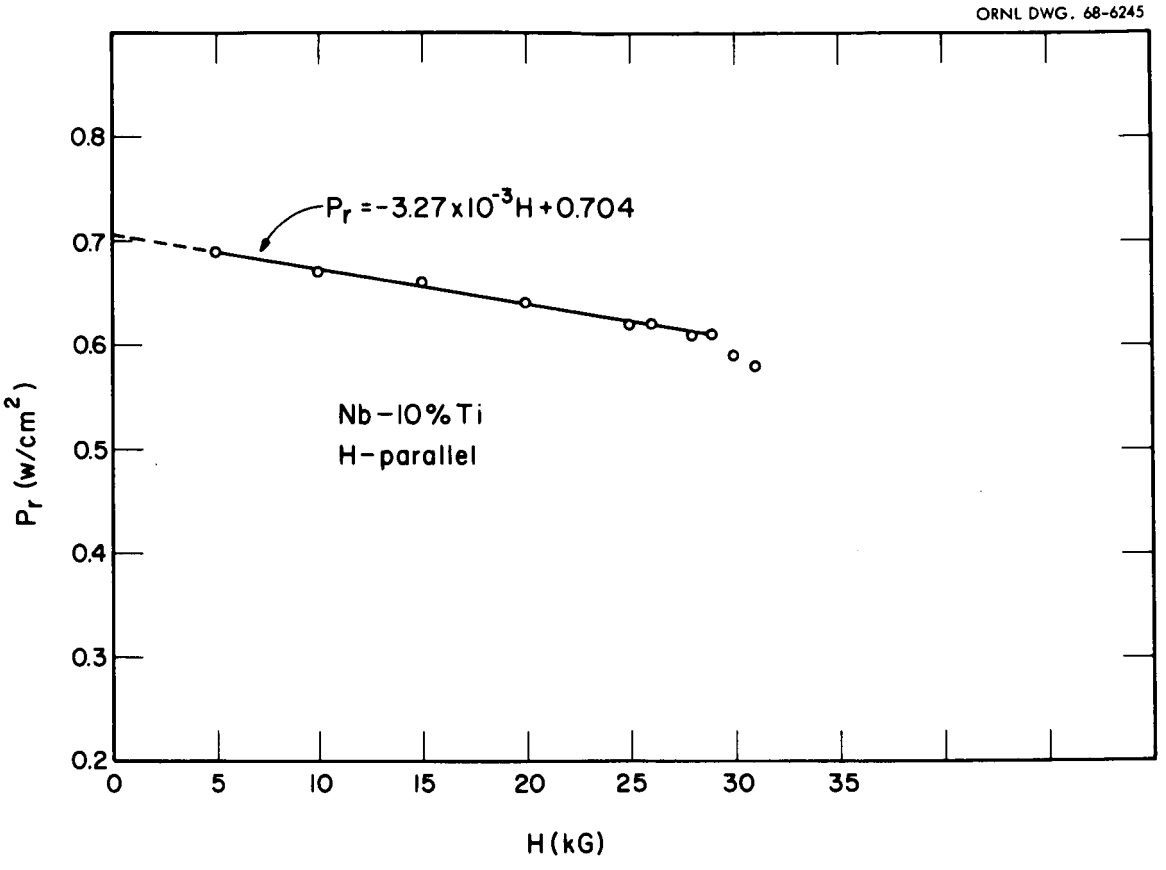

Fig. 14 Recovery power, $P_r = V_r I_r$, vs parallel magnetic field. The field dependence of P_r is shown for $T_b = 4.2$ K.

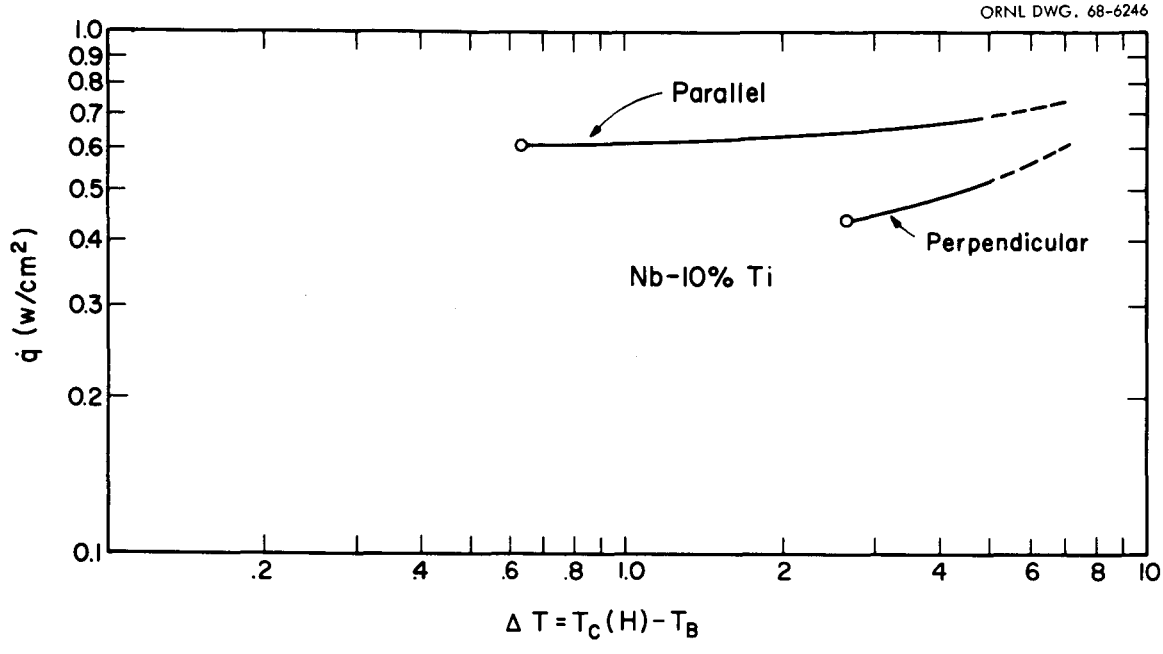

Fig. 15 Log of power vs log of temperature difference between surface and helium bath for the film boiling regime at T_b = 4.2 K. The sample with field perpendicular has a "top" and "bottom" surface and with the field parallel it has two "sideways" surfaces.

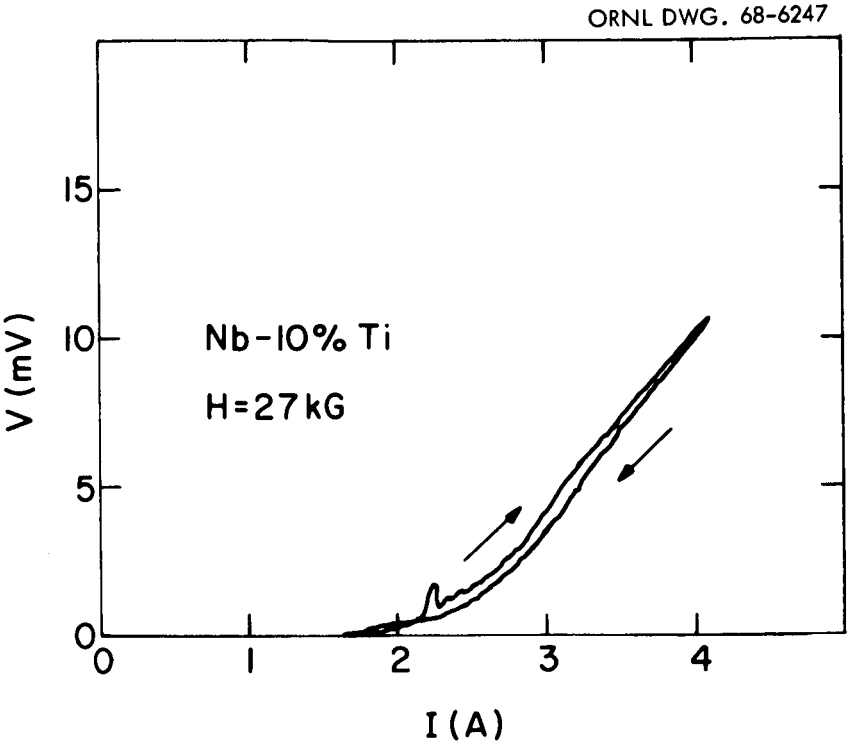

Fig. 16 Voltage vs current at low power levels illustrating the anomaly and hysteresis at T_b = 4.2 K.

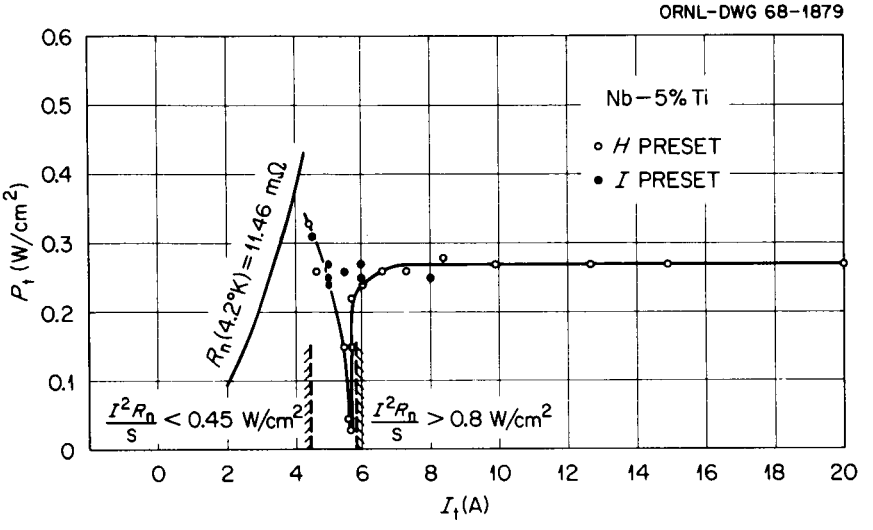

Fig. 17 Take-off power, $P_t = V_t I_t$, vs take-off current. Below I_t = 4.4 A and above I_t = 5.85 A dissipation in a normal zone was less than $\dot{q}_f$ and greater than $\dot{q}_n$, respectively.

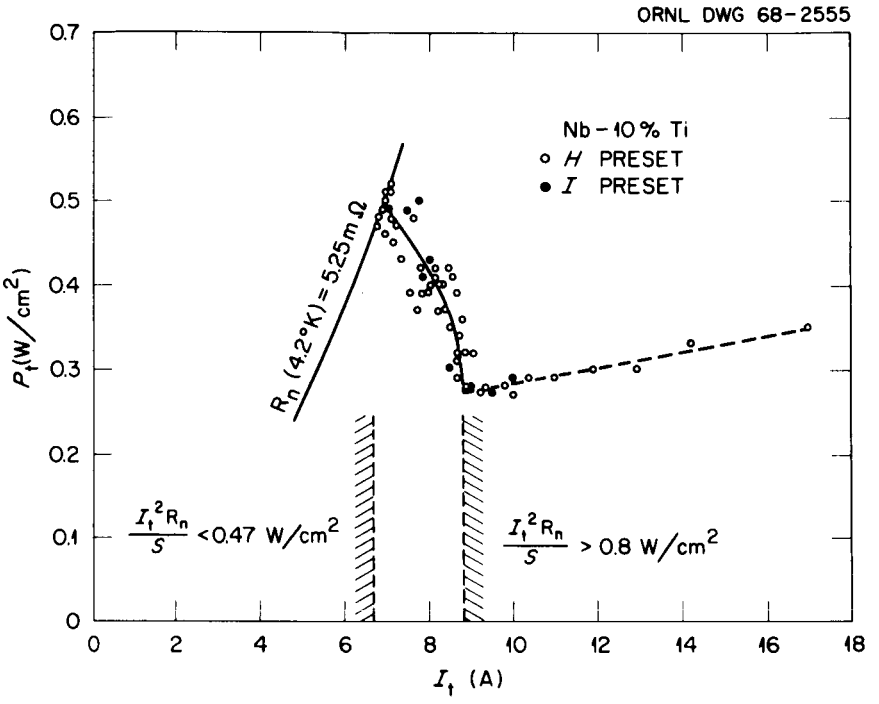

Fig. 18 Take-off power, $P_t = V_t I_t$, vs take-off current. Below I_t = 6.7 A and above I_t = 8.7 A dissipation in a normal zone was less than $\dot{q}_f$ and greater than $\dot{q}_n$, respectively.

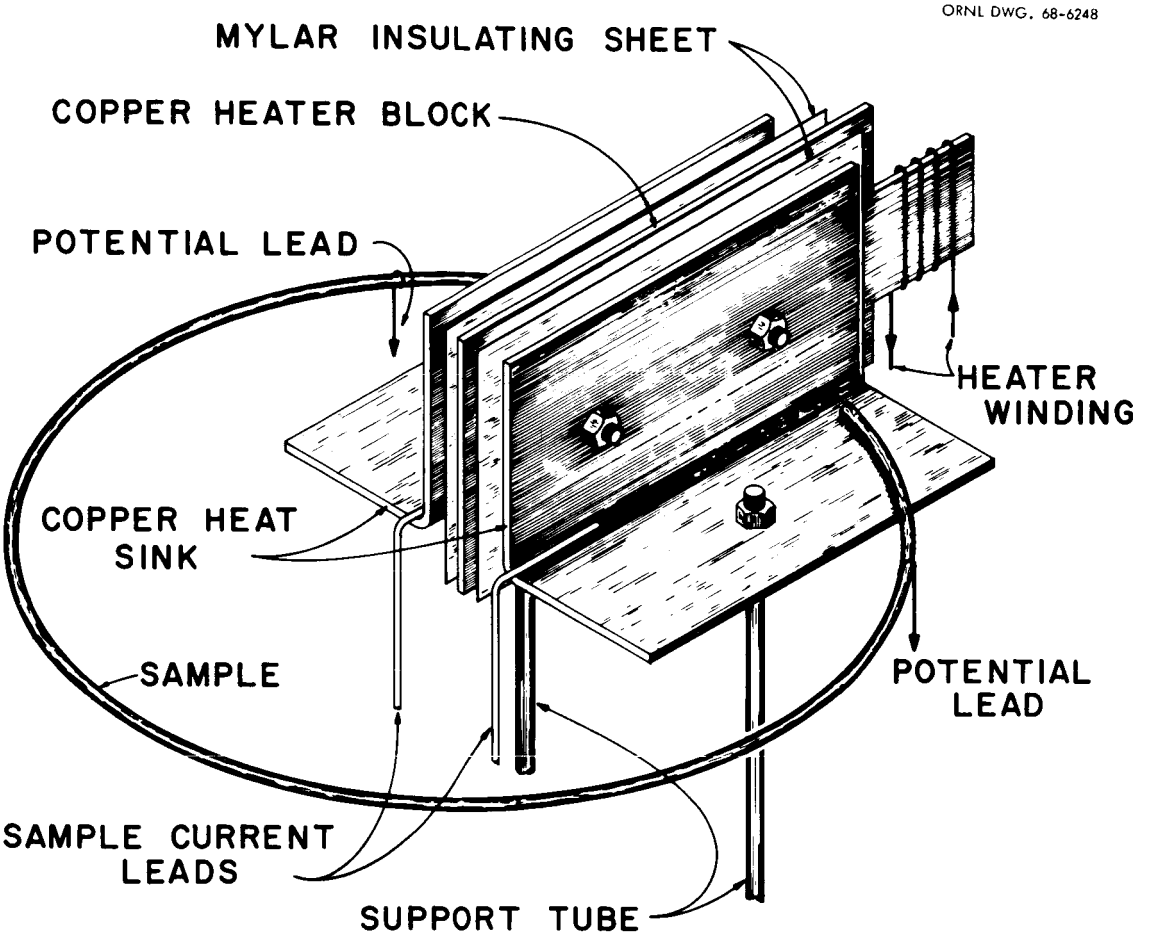

Fig. 19 Experimental apparatus for the measurement of resistance as a function of temperature.

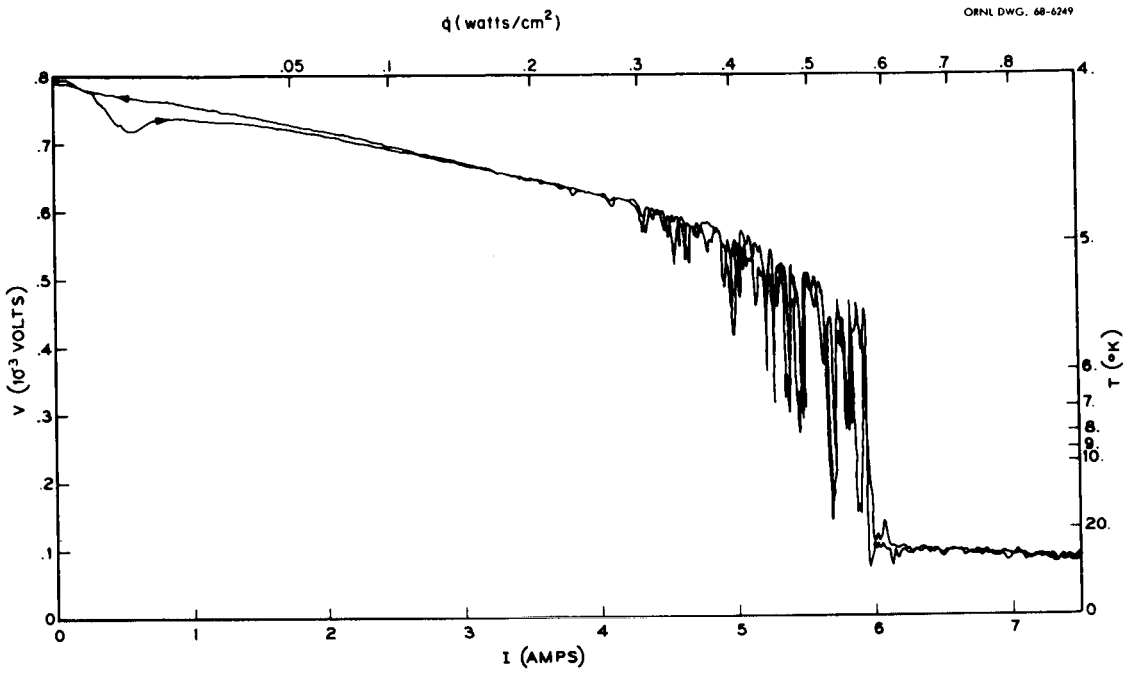

Fig. 20 Heat flux-temperature diagram obtained with an average liquid helium column of 26.5 cm.

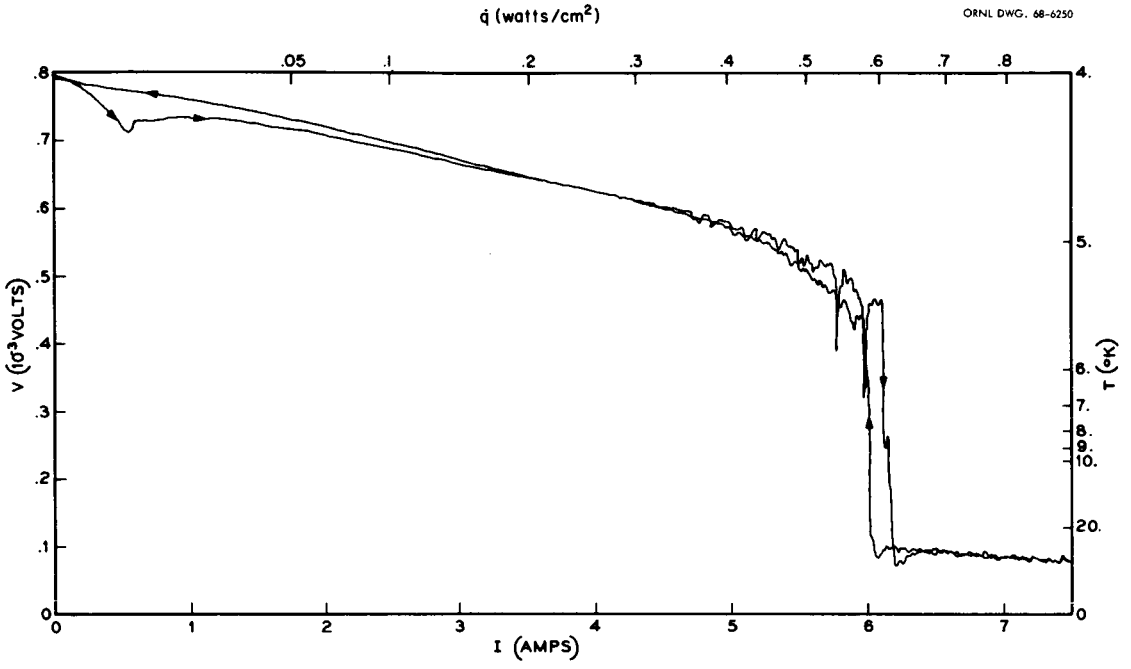

Fig. 21 Heat flux-temperature diagram obtained with an average liquid helium column of 4 cm.

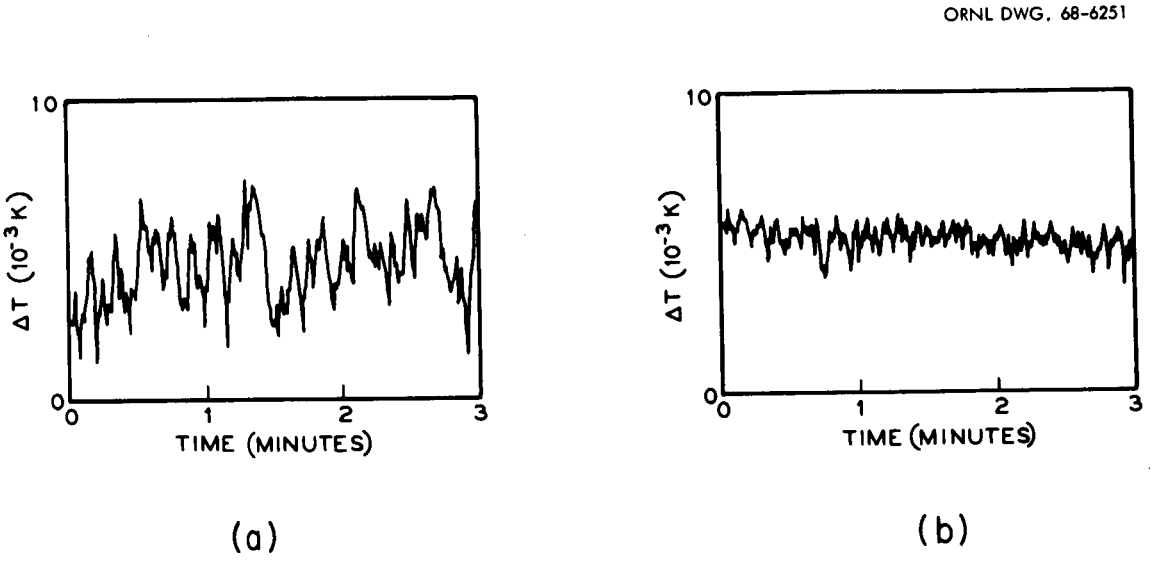

Fig. 22 Temperature fluctuations in liquid helium pumped to 4.0 K.

(a) Average liquid helium column 29 cm;

(b) Average liquid helium column 6.5 cm.

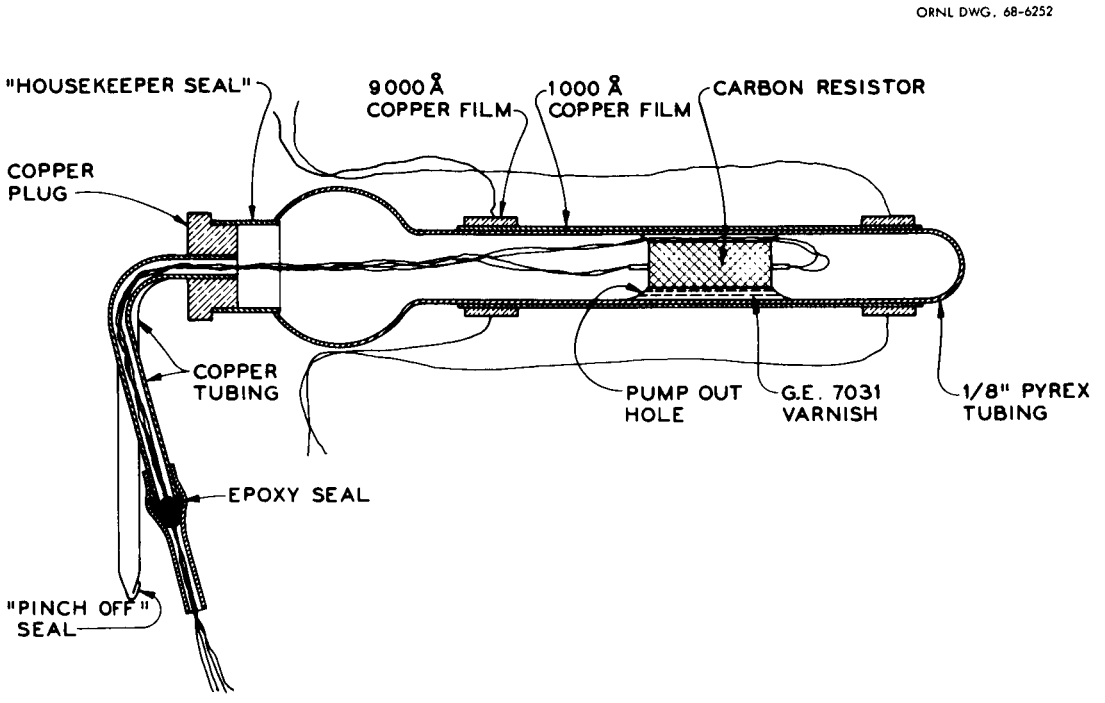

Fig. 23 Thin film probe for heat transfer measurements.

DISTRIBUTION LIST - REPORT JANUARY 1, 1968 TO MARCH 31, 1968

Government Order No. H-29278A

	Addressee	Number of Copies
1.	George C. Marshall Space Flight Center Huntsville, Alabama 35812 Attn: Mr. E. W. Urban	40
2.	U. S. Atomic Energy Commission Oak Ridge Tennessee Attn: Division of Technical Information	15
3.	U. S. Atomic Energy Commission Washington 25, D.C. 20545 Attn: Mr. William C. Gough	3
4.	Princeton University Princeton, New Jersey Attn: Dr. R. G. Mills Mr. P. A. Thompson	2
5.	Lawrence Radiation Laboratory Livermore, California Attn: Dr. C. D. Henning Dr. C. E. Taylor Dr. C. M. Van Atta	3
6.	Los Alamos Scientific Laboratory Los Alamos, New Mexico Attn: Dr. C. F. Hammel Dr. E. L. Kemp Dr. H. L. Laquer Dr. J. L. Tuck	4
7.	Massachusetts Institute of Technology National Magnet Laboratory Cambridge 39, Massachusetts Attn: Dr. H. H. Kolm Mr. D. B. Montgomery Dr. D. J. Rose Dr. E. Maxwell	4
8.	Oak Ridge National Laboratory Oak Ridge, Tennessee Attn: W. F. Gauster 25 Central Research Library 2 Document Reference Section 2 Laboratory Records 2 ORNL-RC 1 ORNL Patent Office 1 Mr. A. J. Miller 1	34

H-29278A

	Addressee	Number of Copies
9.	Brookhaven National Laboratory Upton, New York Attn: Mrs. Jane Garron	10
10.	Argonne National Laboratory Argonne, Illinois Attn: Mr. C. E. Laverick Mr. J. R. Purcell	2
11.	NASA-Lewis Research Center Cleveland, Ohio 44135 Attn: Mr. J. C. Fakan Mr. J. C. Laurence	2
12.	Cryogenic Engineering Laboratory National Bureau of Standards Boulder, Colorado 80301 Attn: Mr. B. Birmingham Dr. R. H. Kropschot	2
13.	RCA Laboratories Harrison, New Jersey Attn: Mr. E. R. Schrader	1
14.	RCA Laboratories Princeton, New Jersey Attn: Dr. G. D. Cody	1
15.	Avco-Everett Research Laboratory 2385 Revere Beach Parkway Everett 49, Massachusetts Attn: Dr. Z. J. J. Stekly	1
16.	General Electric Research & Development Center P. O. Box 8 Schenectady, New York 12301 Attn: Mr. C. H. Rosner Dr. R. W. Schmitt	2
17.	Supercon Division National Research Corporation 9 Erie Drive East Natick, Massachusetts	1

H-29278A

	Addressee	Number of Copies
18.	North American Aviation Atomics International Division P. O. Box 309 Canoga Park, California 91305 Attn: Dr. R. Boom Dr. S. L. Wipf	2
19.	Linde Division of Union Carbide Corporation Speedway Laboratories Indianapolis, Indiana Attn: Dr. D. C. Freeman, Jr.	1
20.	Linde Division of Union Carbide Corporation Tonawanda, New York Attn: Dr. H. Long	1
21.	Cryomagnetics, Incorporated 4955 Bannock Denver, Colorado 80216 Attn: C. N. Whetstone	1
22.	U. S. Atomic Energy Commission Oak Ridge, Tennessee Attn: Laboratory and University Division	1